

# Self-Lubricating, Living Contact Lenses

María Puertas-Bartolomé, Izabook Gutiérrez-Urrutia, Lara Luana Teruel-Enrico, Cao Nguyen Duong, Krupansh Desai, Sara Trujillo, Christoph Wittmann, and Aránzazu del Campo\*

The increasing prevalence of dry eye syndrome in aging and digital societies compromises long-term contact lens (CL) wear and forces users to regular eye drop instillation to alleviate discomfort. Here a novel approach with the potential to improve and extend the lubrication properties of CLs is presented. This is achieved by embedding lubricant-secreting biofactories within the CL material. The self-replenishable reservoirs autonomously produce and release hyaluronic acid (HA), a natural lubrication and wetting agent, long term. The hydrogel matrix regulates the growth of the biofactories and the HA production, and allows the diffusion of nutrients and HA for at least 3 weeks. The continuous release of HA sustainably reduces the friction coefficient of the CL surface. A self-lubricating CL prototype is presented, where the functional biofactories are contained in a functional ring at the lens periphery, outside of the vision area. The device is cytocompatible and fulfils physicochemical requirements of commercial CLs. The fabrication process is compatible with current manufacturing processes of CLs for vision correction. It is envisioned that the durable-by-design approach in living CL could enable long-term wear comfort for CL users and minimize the need for lubricating eye drops.

management, digital medicine, and communication.<sup>[1]</sup> The transfer of this vision into widely accepted user products demands CL materials with the highest and most durable comfort.<sup>[2]</sup> In soft CLs, user comfort depends on the capacity of the CL material to retain moisture, provide high lubrication, and avoid adsorption of tear fluid molecules on the CL surface, among other factors.<sup>[3]</sup> Wettability and water retention in CLs have been significantly improved in commercial CLs by grafting hydrophilic polymer layers, surfactants, or lipids on the surface of the lens (e.g., MoistureSeal, Aquaform or Hydraluxe technologies, among others).<sup>[4]</sup> Alternative academic approaches have been recently suggested based on embedded electronics<sup>[5]</sup> or engraved microchannels<sup>[6]</sup> to transport and retain tear fluid at the eye–lens interface.

The release of wetting and lubricating agents (i.e., poly(vinyl alcohol) (PVA), hydroxypropyl methylcellulose, and hyaluronic acid (HA)) and lipids previously adsorbed or embedded in the lens, is currently the gold standard to improve lubrication and hydrophilicity in CLs and user comfort.<sup>[7]</sup> However, the limited capacity of the CLs to uptake hydrophilic molecules by soaking, and the rapid clearance of components in the tear fluid, limit the duration of the wetting and lubrication effects to a few hours in commercial CLs. CL wearers that experience discomfort are therefore dependent on the regular use of eye drops to externally provide the lubricant agent. Considering the increasing incidence of dry eye symptoms with an aging population and the increased use of digital formats,<sup>[8]</sup> alternative solutions for long-term supply of wetting, and lubricant agents are to be developed.

A promising academic alternative for extending the amount and delivery time scale of a lubricant on a gel surface is the Lubricant-infused surfaces (LIS), inspired by the skin of earthworms.<sup>[9]</sup> In LIS, lubricant molecules are embedded within microdroplets in the bulk of the material and diffuse to the surface to form a self-repairing lubricant film. This strategy has been successfully applied to extend the lubrication of porous and elastomeric surfaces and more recently hydrogel surfaces.<sup>[10]</sup> However, in order to extend the lubrication for the complete lifetime of the material, as in the skin of the earthworm, lubricant reservoirs with a refilling function would be necessary for LIS. In the

## 1. Introduction

Smart contact lenses (CLs) for therapeutic delivery, diagnostics or augmented vision have the potential to revolutionize health

M. Puertas-Bartolomé, L. L. Teruel-Enrico, C. N. Duong, K. Desai, S. Trujillo, A. del Campo  
INM-Leibniz Institute for New Materials  
Campus D2 2, 66123 Saarbrücken, Germany  
E-mail: [aranzazu.delcampo@leibniz-inm.de](mailto:aranzazu.delcampo@leibniz-inm.de)

M. Puertas-Bartolomé, A. del Campo  
Chemistry Department  
Saarland University  
66123 Saarbrücken, Germany

I. Gutiérrez-Urrutia, C. Wittmann  
Institute for Systems Biotechnology  
Saarland University  
Campus A1 5, 66123 Saarbrücken, Germany

 The ORCID identification number(s) for the author(s) of this article can be found under <https://doi.org/10.1002/adma.202313848>

© 2024 The Authors. Advanced Materials published by Wiley-VCH GmbH. This is an open access article under the terms of the [Creative Commons Attribution-NonCommercial](#) License, which permits use, distribution and reproduction in any medium, provided the original work is properly cited and is not used for commercial purposes.

DOI: 10.1002/adma.202313848

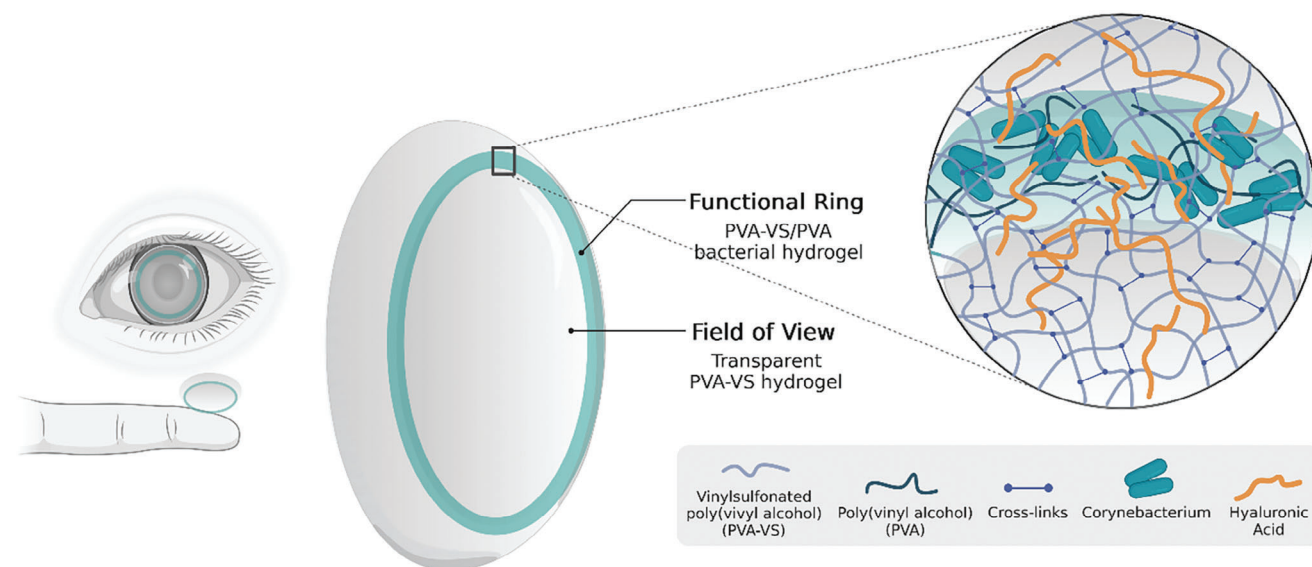


**Figure 1.** Design and composition of the living self-lubricating CL. Created with BioRender.com.

earthworm, this is fulfilled by skin-embedded glands that self-produce lubricant molecules. In a CL scenario, self-replenishable lubricant depots would allow countering the rapid and continuous clearance and dilution of the lubricant in the tear layer during wear time.

Here we propose a design for long-term, self-lubricating CLs based on embedded self-replenishable reservoirs that can autonomously produce and release a lubricating agent (Figure 1). The reservoirs are living biofactories programmed to produce and release HA, the natural wetting and lubrication agent used as the gold standard in ophthalmic applications. The release is passively regulated by the composition and crosslinking of the hydrogel network. This controls the activity of the biofactories and the diffusion rate of the lubricant and therefore determines the rate of self-replenishment and renewal of the surface layer. The engineered living hydrogel with self-lubricating properties supports a long-term delivery of HA and can be processed as a CL laboratory prototype. We envision that this design can be applied to new CLs with durable wetting and lubrication.

## 2. Results

### 2.1. Design of the Living Contact Lens (CL)

The envisioned self-lubricating, living CL is a soft, hydrogel lens that contains bacteria embedded at the rim of the device, outside of the vision area (Figure 1). In this work, the biofactory is metabolically engineered from the soil-inhabiting, Gram-positive *Corynebacterium glutamicum*. This microbe forms no endotoxins and is generally recognized as safe (GRAS), allowing the synthesis of a range of commercial products granted GRAS status by the United States Food and Drug Administration for the food and pharmaceutical industries,<sup>[11]</sup> including amino acids, vitamins, and bioactives.<sup>[12]</sup> Furthermore, it serves as a model for taxonomically related organisms.<sup>[13]</sup> In our work, *C. glutamicum*

DSM 20300 is taken as a working model for *Corynebacterium mastitidis*, a taxonomically related commensal microbe of the human eye that has already demonstrated beneficial properties as a probiotic.<sup>[14,15]</sup> The wild type was metabolically engineered to synthesize and secrete HA. In a first step, we eliminated the native *ldhA* gene encoding lactate dehydrogenase from the genome in order to prevent potential accumulation and secretion of lactate in case of oxygen-limiting conditions. A positive clone, obtained after two recombination events, yielded the shortened PCR fragment, expected for the deletion. After validation of the correct modification using Sanger sequencing, the mutant was designated *C. glutamicum*  $\Delta$ *ldhA*. Subsequently, we expressed the two-gene biosynthetic cluster *hasAB* from *Streptococcus equisimilis*, encoding HA synthetase and UDP-glucose dehydrogenase, respectively, in the mutant to enable HA production. The heterologous operon comprised the constitutive promoter  $P_{tuf}$  upstream of *hasAB* to enable constitutive expression in the host. When grown in suspended culture, the strain formed and excreted HA which could be quantified in the supernatant (Figure S1, Supporting Information).

The embedding hydrogel contains PVA and PVA functionalized with vinyl sulfone (VS) groups.<sup>[16]</sup> (Figure S2, Supporting Information). The VS functionalization allows covalent crosslinking of the chains to form a stable network. The addition of sacrificial, non-crosslinkable PVA allows modulation of the porosity of the network. PVA is a clinically approved hydrogel for use in CLs.<sup>[17]</sup> and is also used for probiotic encapsulation.<sup>[18–20]</sup> PVA-VS/PVA hydrogels were prepared by the polymerization of PVA-VS and PVA mixtures using LAP as photoinitiator. In screening experiments, solutions with 5–10% w/v concentration of PVA-VS (177 kDa) with a degree of VS functionalization of  $1.5 \pm 0.2\%$  formed transparent and mechanically stable hydrogels. Preliminary encapsulation experiments with *C. glutamicum* demonstrated that the bacterium was able to grow inside these hydrogel compositions (data not shown). This preliminary information narrowed the useful compositional range for the design of the

**Table 1.** Physicochemical properties of PVA-VS/PVA hydrogels and the commercial PVA-based Focus Dailies CL (Alcon) measured in STF.

Material	Polymer content [% w/v]	Equilibrium water content (EWC) [%]	Oxygen permeability $D_k$ [barriers] <sup>a)</sup>	Water contact angle [°]	Transmittance [%] <sup>b)</sup>	Refractive index	Storage modulus $G'$ [kPa] <sup>c)</sup>
Focus Dailies	–	61 ± 3	19 ± 2	28 ± 4	>99	1.380	15.6 ± 0.2
PVA-VS/PVA 100:0	10	87.5 ± 0.9	53.9 ± 2.4	29 ± 3	99.1 ± 0.5	1.336	17.9 ± 0.1
PVA-VS/PVA 100:0	5	86.1 ± 0.6	50.9 ± 1.5	23 ± 7	98.4 ± 0.6	1.334	2.2 ± 0.3
PVA-VS/PVA 99:1	5	86.6 ± 1.1	52.1 ± 2.8	22 ± 3	98.4 ± 0.3	1.333	1.6 ± 0.2
PVA-VS/PVA 95:5	5	85.3 ± 0.5	49.4 ± 1.1	23 ± 1	98.7 ± 0.8	1.334	1.5 ± 0.1

<sup>a)</sup> Calculated from EWC measurements; <sup>b)</sup> Value at 600 nm; <sup>c)</sup> Obtained from time sweep measurements.

living CL. The properties of the final hydrogel formulations and the behavior of the embedded bacteria are specified in the next sections.

## 2.2. Physicochemical Properties of the Hydrogel Matrix

Solutions of 10% w/v PVA-VS and 5% w/v PVA-VS/PVA precursors with PVA-VS/PVA ratios of 100:0, 99:1, and 95:5 (Table 1) formed hydrogels within seconds by exposure to light at 365–480 nm (6 mW cm<sup>-2</sup>), according to rheology experiments (Figure S3a, Supporting Information). We used an irradiation time of 120 s (420 nm, 6 mW cm<sup>-2</sup>) for gel formation to ensure full conversion of the VS-mediated crosslinking reaction. At this wavelength, exposure times of 30–300 s at an irradiance of 6–10 mW cm<sup>-2</sup> are compatible with living bacteria.<sup>[21–23]</sup> The 10% w/v PVA-VS hydrogel showed a shear modulus ( $G'$ )

of 17.9 ± 0.1 kPa, close to  $G'$  of commercial PVA CLs (Table 1, Figure S3b–d, Supporting Information). By reducing the PVA-VS content or by replacing a fraction of the PVA-VS by PVA, softer hydrogels were obtained (Table 1). Other physicochemical properties of relevance for CLs (oxygen permeability, transmittance, etc.) measured in simulated tear fluid (STF) were in the range of commercial PVA-based CL (Focus Dailies, Alcon), as shown in Table 1. Images of the obtained hydrogel lenses are shown in Figure 2a.

We evaluated hydrogel properties of relevance for bacterial encapsulation and HA release, i.e., the long-term stability of the hydrogel in STF and the diffusion rate of large molecules through the hydrogel, which indirectly reflects the porosity of the network. All hydrogels retained their shape for at least 21 days in STF. GPC analysis of the supernatant (Figure 2b) showed no PVA release from 5% w/v PVA-VS/PVA 100:0 hydrogels, indicating that the PVA-VS chains were covalently attached or at least physically

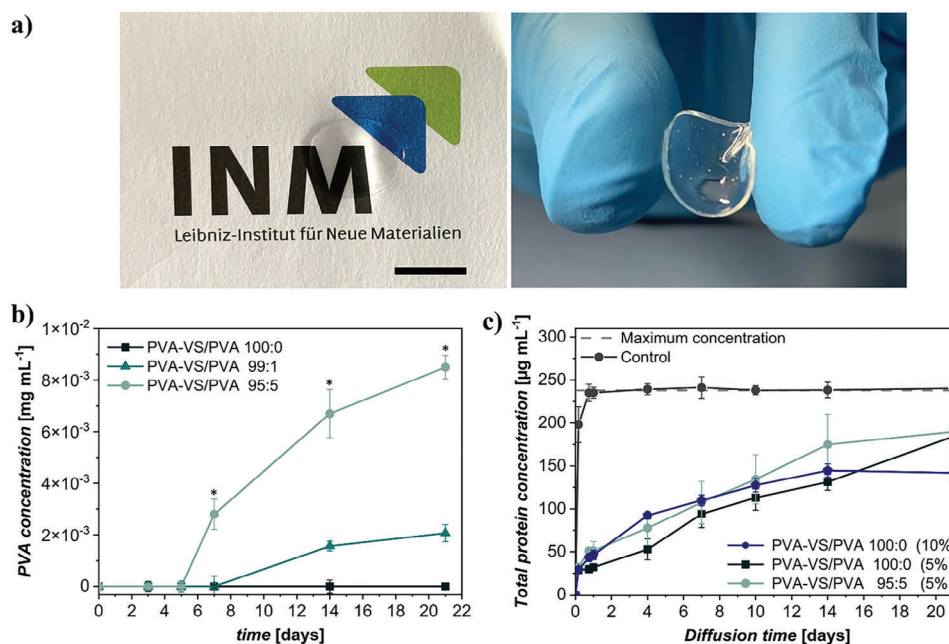


**Figure 2.** a) Transparent PVA-VS/PVA 100:0 hydrogel discs. Scale corresponds to 1 cm. b) Cumulative PVA release from 5% w/v PVA-VS/PVA hydrogels after incubation in STF at 30 °C for 3, 5, 7, 14, and 21 days as obtained from GPC measurements. The GPC curves are shown in Figure S4 (Supporting Information). ANOVA of the results for PVA-VS/PVA hydrogels at each time point was performed at the significant level of  $*p < 0.05$ . c) Protein diffusion kinetics through PVA-VS/PVA hydrogels. A mixture of proteins with molecular weights in the range of 12.3–160 kDa were used for the study. Protein concentration was measured by BCA assay. In the control sample, no hydrogel was used (free diffusion). The dotted line represents the maximum concentration. Complementary data are shown in Figure S5 (Supporting Information) and Table 2.

**Table 2.** Time point at which individual proteins became visible in the electrophoresis gel in the diffusion experiment in Figure S5 (Supporting Information). The table also indicates the molecular weight of the proteins used for the experiment and the band assignment in Figure S5b (Supporting Information).

Protein	$M_w$ [kDa]	Band $M_w$ [kDa]	Diffusion time		
			PVA-VS/PVA 95:5 (5%)	PVA-VS/PVA 100:0 (5%)	PVA-VS/PVA 100:0 (10%)
Cytochrome C	12.3	12.3	4 h	4 h	4 h
Myoglobin equine	17.8	17.8	4 h	4 h	4 h
Chymotrypsinogen A	25	25	4 h	4 h	4 h
Albumin egg	45	45	4 h	1 day	1 day
Albumin bovine (BSA)	67	67	4 h	1 day	14 day
Aldolase	160	40 <sup>a)</sup>	4 h	14 day	–

<sup>a)</sup> The band corresponding to Aldolase was detected at 40 kDa ( $M_w$  of its subunits) due to the denaturation of the protein caused by the dodecyl sulfate.

entrapped in the network. In contrast, 99:1 and 95:5 PVA-VS/PVA hydrogels released part of the PVA to the supernatant (<20% of the initial amount) after a few days. The molar mass distribution of the eluted polymer was the same as of PVA precursor (Figure S4, Supporting Information), indicating that only non-crosslinked PVA was released from the hydrogels.

To study the porosity of the network, we quantified the diffusion rate of proteins with molecular weight between 12.3 and 160 kDa through hydrogel films crosslinked within the insert of a trans-well plate (Figure S5a, Supporting Information). Using the BCA assay (Figure 2c) and gel electrophoresis. All proteins were able to diffuse through the 5% w/v hydrogels, indicating that the pores of the network are larger than 160 kDa. Differences in diffusion kinetics as a function of protein size were observed (Figure S5b, Supporting Information and Table 2). Proteins with molecular weight <25 kDa diffused through the hydrogels within 4 h. Proteins with size >25 kDa required 4 h to diffuse through the hydrogel that included non-crosslinked PVA, and 1 to 14 days when the PVA-VS content increased from 5% to 10% w/v. In summary, the developed hydrogels allow slow diffusion of medium to large molecules. The diffusion rate is dependent on the protein size and can be adjusted by tuning the content and the fraction of PVA-VS and PVA in the hydrogel.

### 2.3. Preparation of the Living Hydrogel and Functionality of the Embedded *C. glutamicum*

Bacteria-laden hydrogels were prepared by mixing a suspension of *C. glutamicum* with 5% w/v PVA-VS/PVA 95:5 precursor solutions in culture medium and photocrosslinking in a mold. The contact time of the bacteria and the precursors before crosslinking is 1 min. It is not expected that polymer chains with molecular weight 177 kDa penetrate through the membrane of the Gram-positive bacteria in this time scale.<sup>[24]</sup> Therefore, we do not expect the bacteria to be crosslinked to the network, only trapped in it. The growth of bacteria in the hydrogel during incubation in medium for 21 days at 30 °C was monitored by fluorescence imaging after Live/Dead staining (Figure 3a). This time scale was selected as representative for the life time of a reusable CL (weekly to monthly lenses). We imaged a 132.12 × 132.12 × 18 μm volume at the central part of the hydrogel to avoid interfacial effects from the walls of the well. Initially, individual bacteria at

low density and homogeneously distributed in the gel were observed. During incubation, bacteria proliferated within the hydrogel (Figure 3a and Figure S6, Supporting Information). Bacteria growth, estimated by image analysis of the volume occupied by live bacteria in the hydrogel over time, showed and induction, growth and a steady state phase over several days (Figure 3b). The viability of the biofactories inside the hydrogel was high for the 21 days (Figure 3a,c). Gels remained stable during the 3 weeks of incubation and the bacteria neither grew nor escaped from the hydrogel into the medium, which is important for safety requirements (Figure S7, Supporting Information). We evaluated the metabolic activity of the bacteria in the hydrogels by quantifying the ATP concentration in the encapsulated population using the CellTiter-Glo 3D viability assay (Figure 3d and Figure S8, Supporting Information).<sup>[25,26]</sup> An increase in the average metabolic activity measured was observed during the first week, followed by a constant value at longer times. In conclusion, the 5% w/v PVA-VS/PVA 95:5 hydrogel supports encapsulation, spatially contained growth and activity of *C. glutamicum* for at least three weeks.

The induction phases of the bacteria population within the hydrogels occur within the time scale of several days, whereas these phases in suspension take hours (Figure S9a, Supporting Information). The slower growth rate can be associated with the spatial confinement imposed by the 3D hydrogel network, as suggested in preliminary experiments (Figure S9b, Supporting Information) and supported by findings reported for other encapsulated bacteria strains.<sup>[21,23,27,28]</sup> When forming a biofilm, *C. glutamicum* has also been shown to grow slower than in suspension.<sup>[29,30]</sup> According to reported work,<sup>[30]</sup> the slow growth mode is accompanied by higher cell tolerance and viability, which would be favorable in an application scenario. In summary, the developed PVA-VS/PVA hydrogels represent a functional and safe platform for the encapsulation of *C. glutamicum*.

### 2.4. Release of Hyaluronic Acid (HA) from the Living Hydrogel

To assess the long-term capacity of encapsulated *C. glutamicum* to release HA, the 5% w/v bacterial hydrogels were incubated in medium for 21 days, with medium changes on days 7 and 14. The cumulative release of HA was quantified by

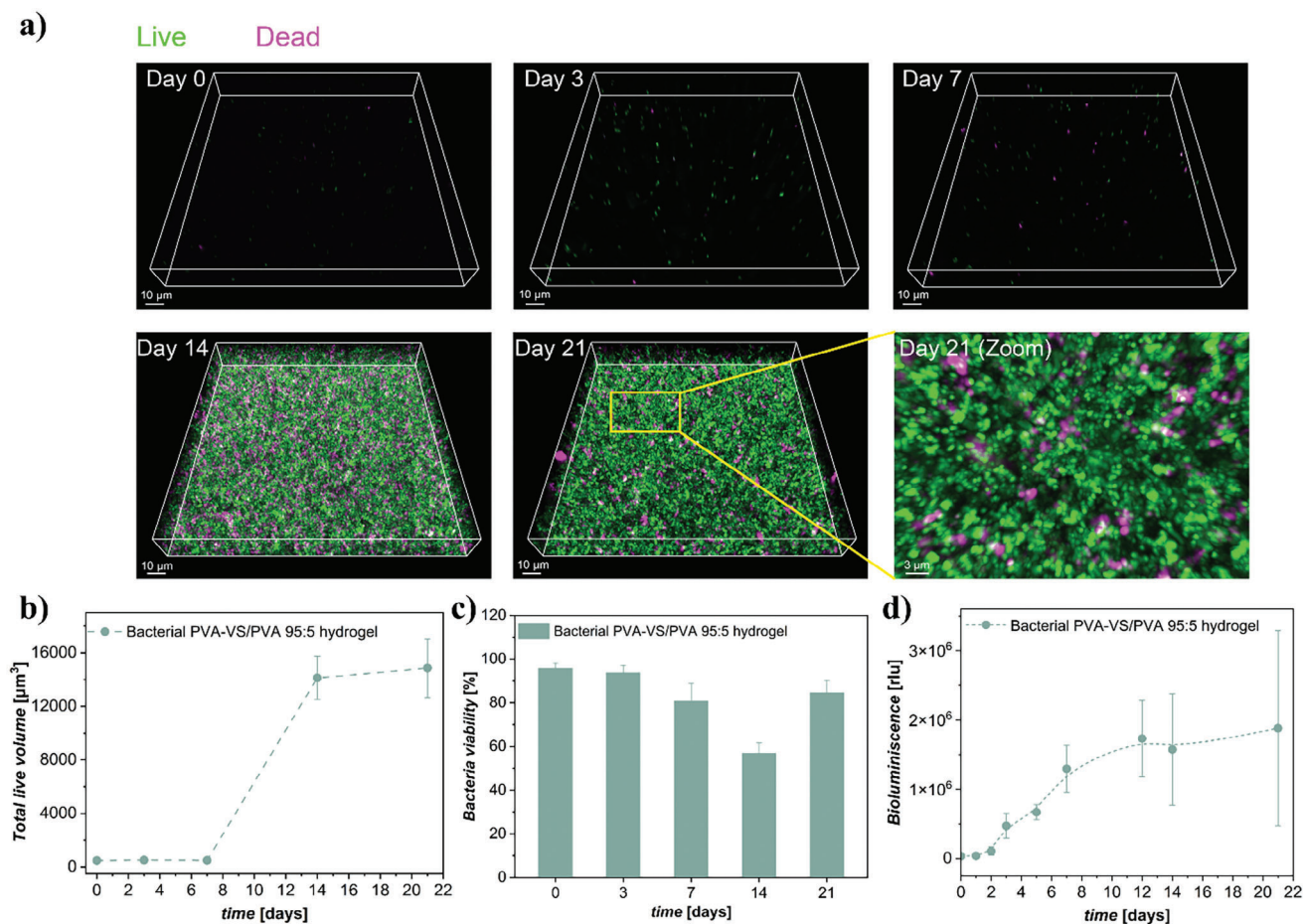


**Figure 3.** a) Representative confocal fluorescence microscopy images of 5% w/v PVA-VS/PVA 95:5 bacterial hydrogels after 0, 3, 7, 14, and 21 days of incubation in BHI medium at 30 °C and Live/Dead staining. Medium was exchanged on days 7 and 14. Represented data corresponds to  $N = 1$ , the experiment was performed at least in triplicate. An independent experiment ( $N = 2$ ) is represented in Figure S6 (Supporting Information). Live bacteria appear in green and dead bacteria in magenta. Images of a size of  $(xy)$   $132.12 \times 132.12 \mu\text{m}$  and Z-stacks of  $18 \mu\text{m}$  were acquired. b) Volume fraction occupied by viable bacteria within PVA-VS/PVA 95:5 hydrogels at 0, 3, 14, and 21 days quantified from Live/Dead image analysis using Imaris software. c) Viability of encapsulated bacteria within PVA-VS/PVA 95:5 hydrogels at 0, 3, 14, and 21 days quantified from Live/Dead image analysis using Imaris software as the percentage of viable cells compared to the total number of cells. d) ATP quantification of bacteria encapsulated in PVA-VS/PVA 95:5 hydrogels during incubation for 21 days in BHI medium. The CellTiter-Glo 3D bioluminescence assay was used for quantification. Medium was exchanged on days 7 and 14. Represented data corresponds to  $N = 1$ , the experiment was performed at least in triplicate, and average and standard deviation are given. An independent experiment ( $N = 2$ ) is represented in Figure S8 (Supporting Information), presenting a batch-to-batch variability while a similar trend is obtained.

GPC analysis of the supernatant at different time points between 3 h and 21 days (Figure 4a). HA with a molecular weight of 30–70 kDa was detected in the supernatant of the hydrogel after 14 h of incubation (Figure S10, Supporting Information). This result confirms the ability of encapsulated *C. glutamicum* in PVA-VS hydrogels to produce and release HA. We note that the release of HA in *C. glutamicum* cultures is detected already after 8 h (Figure S1, Supporting Information). The delayed detection of HA in the hydrogel supernatant is presumably due to the slower growth of the encapsulated bacteria population or the slow diffusion through the hydrogel network. The HA concentration in supernatant continuously increased during the 21 days of incubation, which agrees with the retained metabolic activity detected in the ATP assay. The release rate can be controlled by modulating the covalent crosslinking and the medium used. As seen in

Figure 4b, the addition of non-crosslinked PVA in the hydrogel network (5%) can lead to higher HA release, presumably attributed to the faster growth of the organisms, as suggested in preliminary experiments (Figure S9b, Supporting Information), and faster molecular diffusion in less crosslinked networks.

## 2.5. Self-Lubrication Properties of the Living Hydrogel

The self-lubrication properties of the bacterial hydrogels were quantified by measuring the friction coefficient of PVA-VS/PVA 95:5 hydrogel discs loaded with HA-producing *C. glutamicum*. As controls, we used hydrogels containing wild type *C. glutamicum* which did not produce HA. We used a rheology-based methodology<sup>[31,32]</sup> in which a hydrogel disc is attached to

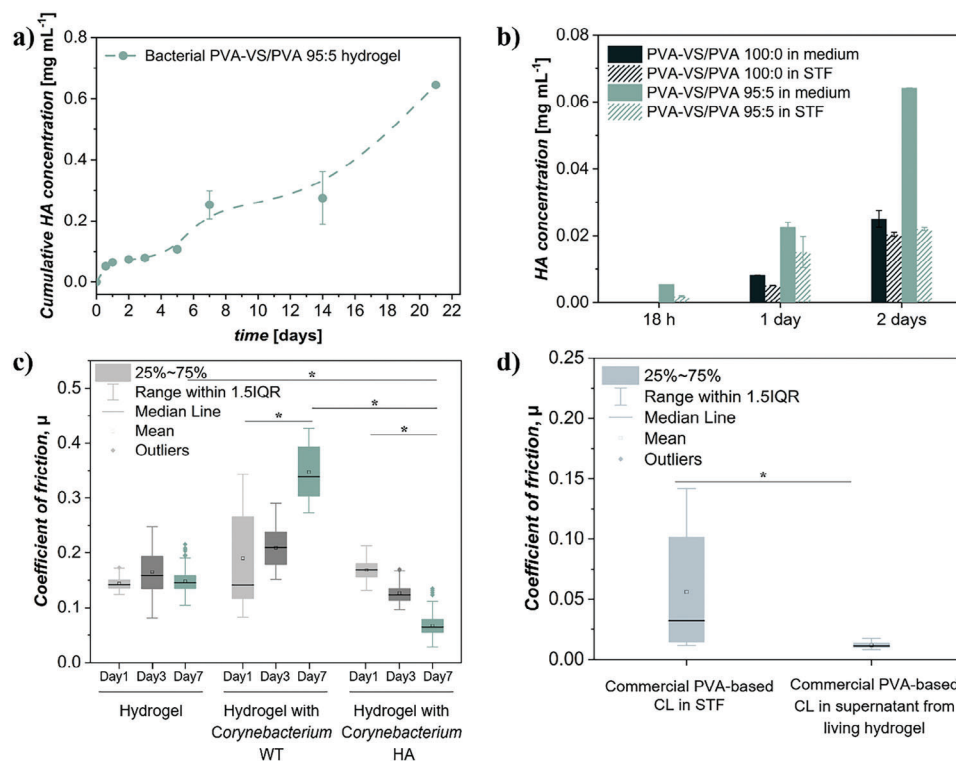


**Figure 4.** a) Cumulative HA concentration released from bacterial PVA-VS/PVA 95:5 hydrogels during 21 days incubation in BHI medium and medium exchange on days 7 and 14 (samples from Figure 3) measured by GPC analysis of the supernatant. Represented data corresponds to  $N = 1$ , experiment was performed at least in triplicate, and average and standard deviation are given. b) Cumulative HA concentration released from bacteria PVA-VS/PVA 95:5 and 100:0 hydrogels after different incubation times in BHI medium or STF measured by GPC analysis of the supernatant.  $N = 1$ , the experiment was analyzed in triplicate, and average and standard deviation are given. The GPC curves are shown in Figure S10 (Supporting Information). c) Coefficient of friction of PVA/PVA-VS 5:95 hydrogels without bacteria, containing *C. glutamicum* wild type, or containing the engineered HA-producer *C. glutamicum*, measured in a rotating rheometer. Measures were performed with hydrogels incubated for 0, 3, and 7 days.  $N = 2$ , data were performed at least in duplicate, and average and standard deviation are given. Box charts indicate 75 and 25 percentile values, whiskers indicate standard deviation values, and  $p$ -values are calculated using one-way ANOVA at the significant level of  $*p < 0.05$ . d) Coefficient of friction of commercial PVA-based Focus Dailies CL (Alcon) measured in a rotating rheometer in the presence of STF or the supernatant of the bacterial hydrogel releasing HA during 7 days.  $N = 2$ , data were performed at least in duplicate, and average and standard deviation are given. Box charts indicate 75 and 25 percentile values, whiskers indicate standard deviation values, and  $p$ -values are calculated using one-way ANOVA at the significant level of  $*p < 0.05$ .

the upper plate of the rheometer and the torque is measured against a steel bottom plate in the presence of the corresponding supernatant while an angular force is applied.<sup>[33]</sup> This methodology does not take into account the curvature of the eye surface but is considered sufficient to test the relative differences between the hydrogels. We compared the friction coefficient of the hydrogels in the presence of the supernatant after incubation for 0, 1, and 7 days (Figure 4c and Figure S11a–c, Supporting Information), from which no HA, a low or a medium concentration of HA was expected (Figure 4a). On day 0, all hydrogels showed a similar friction coefficient (0.14–0.21). The coefficient of friction of control hydrogels without bacteria did not vary after incubation for 1 or 7 days. Hydrogels containing the *C. glutamicum* wild type showed a progressive increase in the friction coefficient on day 7, up to a value of 0.30–0.40. This is presumably due to the release of metabolites and proteins that can interact with the hydrogel. In contrast, the coefficient of friction of hydrogels containing the engineered, HA-producing *C. glutamicum* gradually decreased with the incubation time in a significant way and reached 0.05–0.09 on day 7. We attribute this decay

to the presence of HA in the supernatant and eventually on the surface of the hydrogel, and the consequent self-lubrication effect. However, we cannot exclude some contribution from a softening of the PVA-VS hydrogel as it gets replenished with PVA. Control friction experiments were performed with the commercial PVA CLs (Focus Dailies) in STF and in 7-day supernatant from HA-releasing bacteria (Figure 4d and Figure S11d, Supporting Information). Also in this case, the friction coefficient of the CL surface significantly decreased when measured in supernatant, corroborating the lubricating properties of the secreted molecules.

## 2.6. Fabrication of Laboratory Self-Lubricating CL Prototypes

We fabricated laboratory CL prototypes in a two-step molding process (Figure 5a). A ring-shaped PVA-VS/PVA 95:5 hydrogel (5% w/v) containing *C. glutamicum* was first molded (10 mm diameter). The ring was embedded in a second molding step into 10% w/v PVA-VS hydrogel with a CL form. The hydrogel had

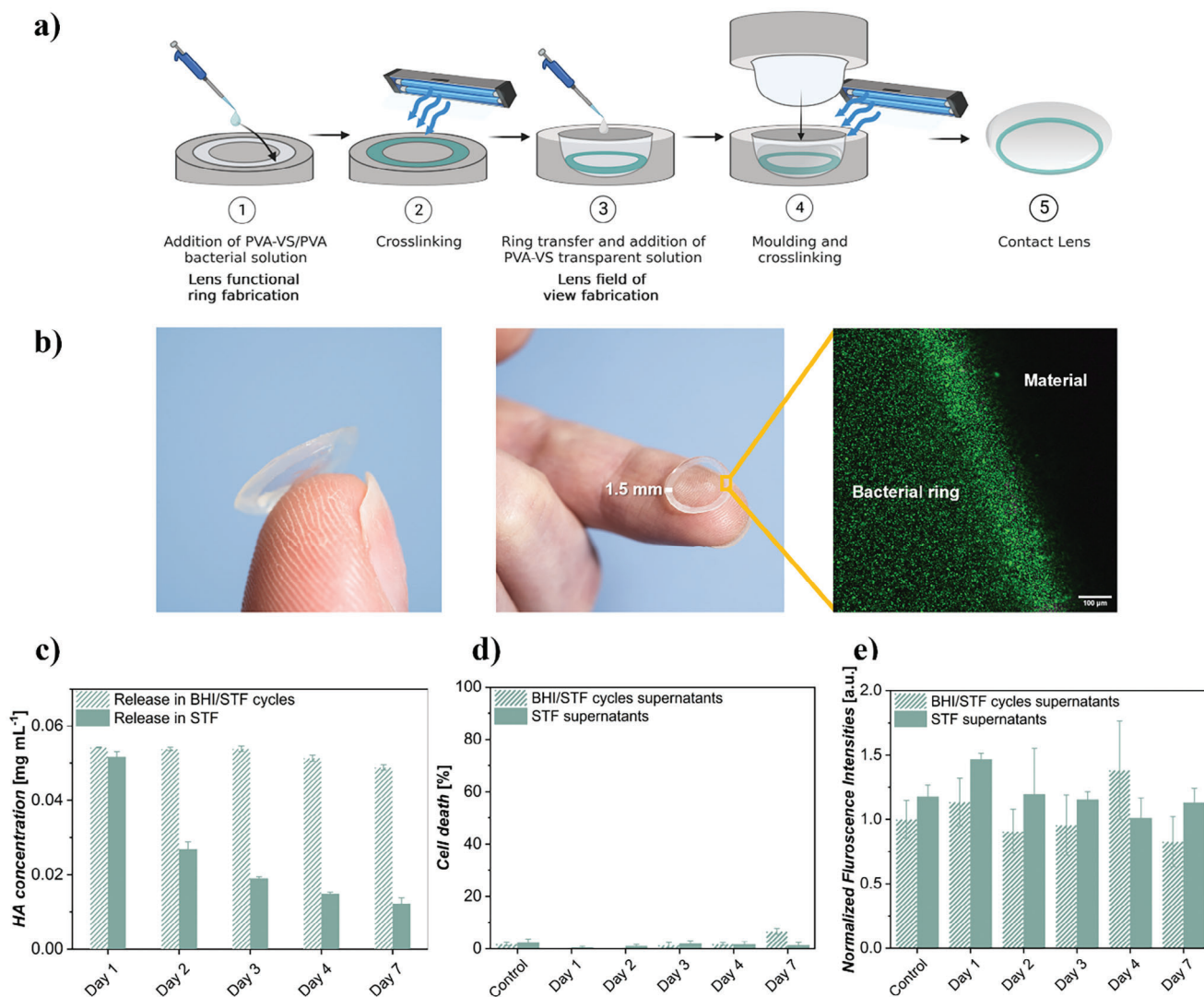


**Figure 5.** a) Schematic illustration of the fabrication process of the bacterial ring-implanted CL. Created with BioRender.com. b) Top side view images of a ring-implanted hydrogel CL (silica gel at 50% w/w was used to improve visualization of the ring), and confocal visualization of encapsulated bacteria on the border of the ring after 7 days of incubation and Live/Dead staining. The live bacteria stained appear in green and the dead bacteria appear in magenta. c) HA concentration released from bacterial ring-CLs after incubation in two nutrition scenarios: release in STF during 7 days, or incubation/release cycles of 16 h in BHI and 8 h in STF respectively during 7 days. Represented data correspond to  $N = 3$ , and average and standard deviation were given. d) Viability (LDH assay) and e) metabolic activity (Alamar Blue) of NIH-3T3 fibroblasts performed after 24 h in contact with bacterial ring-CL supernatant supplementation. CL supernatants were collected after incubation of the CL prototypes in two nutrition scenarios: release in STF during 7 days, or incubation/release cycles of 16 h in BHI and 8 h in STF respectively during 7 days. Controls correspond to cells cultured in cell culture medium. Represented data in (d) and (e) correspond to  $N = 1$ , the experiment was performed in quadruplet, and average and standard deviation were given.

11 mm diameter and 1.5 mm thickness. We used a larger thickness than in commercial CLs to facilitate manipulation during the experiments. There is no inherent limitation in the material or the approach preventing adjustment of the protocol to a thinner sample. After crosslinking, mechanically stable and transparent hydrogel CL prototypes were obtained (Figure 5b). When incubated in medium, *C. glutamicum* grew within the ring volume, outside of the vision area (Figure 5b), and no outgrowth or leaking of bacteria were observed (Figure S12, Supporting Information).

CL prototypes were first incubated in BHI medium for 3 days, and HA release was evaluated afterward in two possible “nu-

trition” scenarios (Figure 5c): i) release in STF, and ii) incubation/release cycles of 16 h in BHI and 8 h in STF respectively, which tries to mimic the CL usage time. In both scenarios, a 7-day experimental period was chosen based on HA release results from the previous study (Figure 4a). The released HA was quantified by GPC of the supernatants. In the first case, HA release decreased with time, as expected from a medium with no nutrients. In the second case a constant release of HA was observed, indicating that the cyclic exposure to nutrients can sustain the HA production. This demonstrates that the living CL prototype can provide sustained HA delivery in a scenario that simulates overnight incubation and daily HA release. Altogether, these

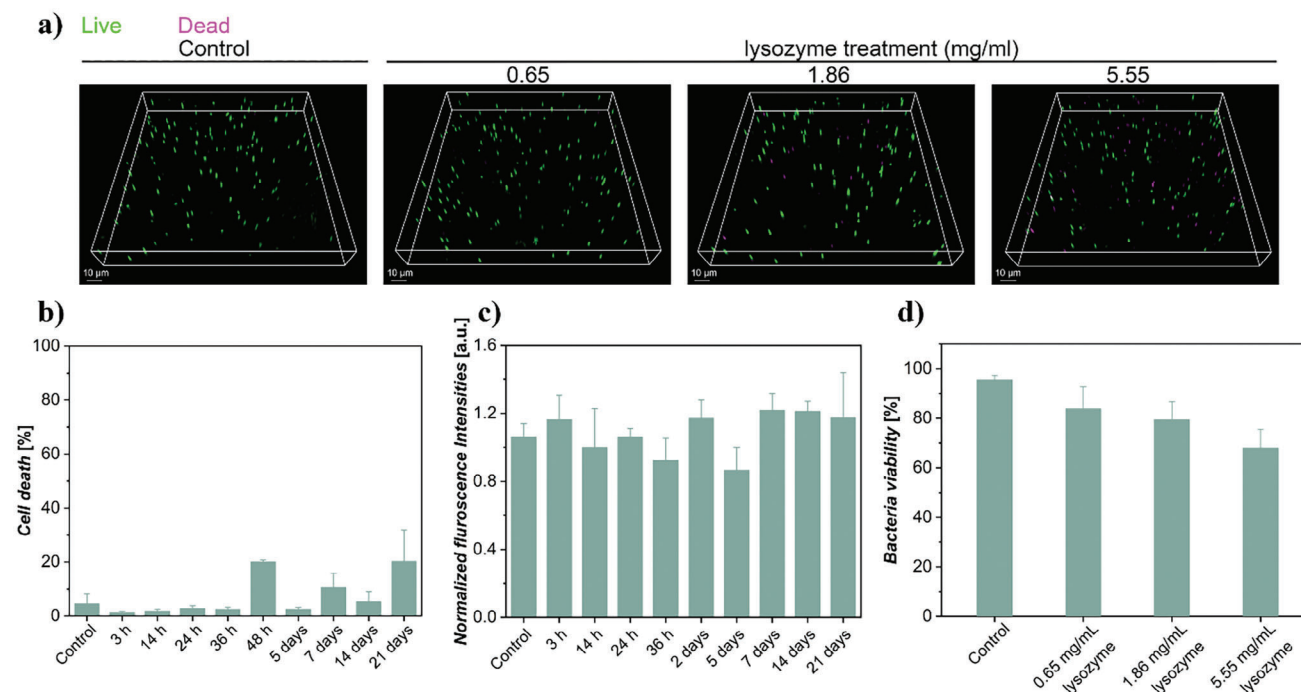


**Figure 6.** a) Representative confocal fluorescence microscopy images of 5% w/v PVA-VS/PVA 95:5 bacterial hydrogels after 24 h of incubation with increasing lysozyme concentrations (0.65, 1.86, and 5.55 mg mL<sup>-1</sup>) at 30 °C and Live/Dead staining. Live bacteria appear in green and dead bacteria in magenta. Images of a size of (xy) 132.12 × 132.12 μm and Z-stacks of 18 μm were acquired. Represented data corresponds to N = 1, the experiment was performed at least in triplicate. b) Viability (LDH) and c) metabolic activity (Alamar Blue) of NIH-3T3 fibroblasts performed after 24 h in contact with bacterial-PVA-VS/PVA 95:5 hydrogels supernatant supplementation. Supernatants from bacterial-PVA-VS/PVA 95:5 hydrogels were collected after incubation in BHI medium at 30 °C for increasing times between 3 h and 21 days (samples from Figure 3). Controls correspond to cells cultured in cell culture medium. Represented data correspond to N = 1, experiment was performed in quadruplet, and average and standard deviation were given. d) Cytocompatibility of bacterial-PVA-VS/PVA 95:5 hydrogels after incubation for 24 h with increasing lysozyme solutions (0.65, 1.86, and 5.55 mg mL<sup>-1</sup>). Bacteria viability was calculated using Live/Dead image analysis from (a) using Imaris software as the percentage of viable cells compared to the total number of cells.

results show different alternatives for the replenishing of a living cCL in a possible application scenario.

## 2.7. Cytocompatibility of the Living Hydrogel

In a living CL, bacteria are shielded from direct contact with the eye surface by the PVA-VS/PVA hydrogel matrix. No physical contact is possible between the engineered organisms and the cells on the eye surface but their secretome, such as the produced HA, will be exchanged through the tear fluid. We performed cytocompatibility studies to evaluate the potential cytotoxic effect on host cells of a living CL. An established mouse fibroblastic cell line was selected to test cytotoxicity. NIH-3T3 fibroblasts were incubated with the supernatant from bacteria hydrogels collected after different times of incubation (between 3 h and 21 days) and mixed with cell culture medium. The viability and proliferation of the fibroblasts were quantified by LDH and Alamar Blue assays after 24 h in contact with the supernatant supplementation. High cell viability (>80%, **Figure 6b**) was found for cells in contact with the studied samples according to the LDH assay. No significant difference in cell proliferation was observed between control (medium) and supplementation with supernatants from the bacteria hydrogels, according to the Alamar Blue assay (**Figure 6c**).

The released products from our bacterial hydrogels do not seem to compromise the vitality of fibroblasts within the evaluated concentrations. Fibroblasts were also exposed to supernatants from the CL prototypes collected after incubation in the two nutrition scenarios previously mentioned: release in STF during 7 days, or incubation/release cycles of 16 h in BHI and 8 h in STF respectively during 7 days. High cell viability was also observed after 24 h in contact with the CL supernatant supplementation (**Figure 5d,e**).

In tear fluid, lysozyme is an abundant protein with an antimicrobial function that can degrade the bacteria cell wall.<sup>[34]</sup> Lysozyme is a small protein with 14.5 kDa and can diffuse through the PVA hydrogels.<sup>[34]</sup> We quantified the viability of *C. glutamicum* encapsulated in the hydrogels after 24 h incubation in BHI medium supplemented with lysozyme concentrations between 0.65 and 5.55 mg mL<sup>-1</sup> (from the minimum to the maximum concentration values found in the tear fluid)<sup>[35]</sup> by image analysis after Live/Dead staining (**Figure 6a**). The viability of *C. glutamicum* was >69% for all tested lysozyme concentrations (**Figure 6d**). Note that *C. glutamicum* used in our study was taken as a model of *C. mastitidis* which is a commensal of the eye microbiome and is expected to naturally withstand the presence of lysozyme in the tear fluid.

### 3. Discussion

To extend the wearing time of CLs, HA is commonly delivered to the eye surface either by passive release from the CL or by active application of eye drops. The amount of HA that can be released from a CL is limited by the loading capacity of the CL, and the lubrication effect typically vanishes after a few hours. In HA-containing eye drops, the lubrication effect is limited by the inherent low efficiency of eye drop delivery (<5%) and the rapid turnover of tear fluid. To increase the residence time of HA in the tear layer, ultrahigh molecular weight HA drops.<sup>[36]</sup> (up to 2500 kDa) and CLs with grafted HA-binding protein domains on the surface have been proposed.<sup>[37]</sup> In this context, our self-lubricating CL represents an innovative alternative for long-term lubrication with theoretically no inherent limitation of HA delivery time and control and flexibility in the delivery rate.

The self-lubricating living CL contains an embedded functional ring at the periphery of the lens, outside of the vision area. The reported two-step fabrication process allows the use of different polymer content and crosslinking degree in the embedding ring and in the rest of the lens. The possibility to adjust hydrogel properties independently to support (embedded ring) or prevent (surrounding lens) bacteria growth within a single device is an advantage of this approach since it allows maximizing functional and safety requirements. A growth step of the living CL could be also added as part of the manufacturing process to decrease the delay time in the HA production and obtain a fully operational lens. In addition, the versatility of both the material and the method used allows the ring and lens geometry to be modified as needed. CL production by molding is a standard process in the CL industry, and the embedding of functional components—as in embedded microelectronic devices—seems a feasible method for upscaling. Therefore, the proposed CL design and processing methodology is, in principle, transferrable to a medical product manufacturing context. Although PVA-based CLs are commercially available, the extension of the current design to silicone hydrogels, which show the highest comfort and have the largest market share, is a necessary step for further development of this concept into a real product.

According to the instructions of HA containing eye drops AQuify (CIBA Vision), the recommended daily therapeutic dose of HA is 1  $\mu\text{g}$  per day considering the HA concentration in the drops (0.1% w/v) and estimating a 2% uptake efficiency for eye drop delivery.<sup>[38]</sup> Assuming a HA-uptake efficiency of >50% for CL-mediated HA delivery, the required daily dose delivered by a CL would be 2  $\mu\text{g}$  per day.<sup>[38]</sup> Table S1 (Supporting Information) compares HA release from reported CL prototypes loaded with HA by molecular imprinting,<sup>[39]</sup> entrapment during synthesis,<sup>[40,41]</sup> or soaking.<sup>[41]</sup> methods. With these prototypes, a release of 12–170  $\mu\text{g}$  HA from the hydrogel within 4 days to 7 weeks has been reported. In all cases, >50% of the entrapped HA was eluted within the first hours, and the physical and optical properties of the CL material were affected by HA-loading. These features limit the applicability of these strategies.<sup>[42,43]</sup> HA has also been loaded in a ring enclosed at the periphery of the lens. In this case, 50  $\mu\text{g}$  were released within 15 days and the optical properties were not compromised.<sup>[38]</sup> This approach was combined with drug loading (timotol,<sup>[44]</sup> moxifloxacin HCl,<sup>[45]</sup> or timolol/bimatoprost combinations<sup>[46]</sup>). A cumulative HA release

of  $\approx 10 \mu\text{g}$  in 72 h<sup>[46]</sup> and 96 days<sup>[44,45]</sup> was reported. Higher release was obtained by embedding HA-loaded nanoparticles in the ring, with a HA release up to 285  $\mu\text{g}$  in 14 days (90% of the total loaded amount).<sup>[47]</sup> The self-lubricating CL in our study shows an estimated overall release rate of  $\approx 9.3 \mu\text{g}$  per day which is higher than what is estimated to reach a therapeutic level for HA delivery in tear fluid as previously mentioned.<sup>[38]</sup> In contrast to all the other cases, the release rate can be tuned by adjusting the hydrogel composition and incubation conditions. Increasing the initial amount of embedded biofactories or the content of sacrificial PVA in the hydrogel enabled higher release rates. HA production can be sustained long-time in incubation/delivery cycles that resemble the night/day cycles of CL users. Our experiments showed a sustained release of  $\approx 17 \mu\text{g}$  per day.

In our living CL, the eye surface is protected from direct contact with the bacteria by the PVA-VS/PVA hydrogel matrix. This means that no physical contact occurs between the engineered biofactories and the host cells on the eye surface. This is expected to reduce the possible host immune response. However, the secretome will be exchanged through the tear fluid. This is desired since HA is part of the secretome, and the nutrients in the tear fluid could help maintaining the activity of the biofactories during wear time. However, by-products from the secretome of the engineered bacteria could trigger unwanted reactions from the host cells. Our cytotoxicity experiments show promise for high biocompatibility of the living CL but additional experiments with corneal epithelial cells or tissue samples and with variable bacteria concentrations growth in different conditions are needed to assess the biocompatibility in vitro to prepare follow up in vivo studies.

The self-replenishing biofactories in the living CLs are inspired by the glands in the skin of earthworms, leeches or fishes that secrete their lubricant epidermal mucus. In nature, the clearing and self-renewal of the lubrication layer confers not only low friction, but also long-term protection from biofouling.<sup>[48–51]</sup> This property would also be beneficial for CLs and remains to be tested in the physiological environment. The continuous release flow of HA from living LC could mimic this self-renewal capacity of the lubricating layer and would also help minimize the deposition and accumulation of debris and proteins on the lens surface, which is an important consideration for long-term CL wear.

### 4. Conclusions

We have developed a self-lubricating living CL based on embedded biofactories programmed to continuously produce and release the natural lubricating agent HA. The design includes a ring containing the biofactories which is embedded at the periphery of the CL. The proposed living CL is based on PVA functionalized with VS groups. At 5% concentration, this hydrogel can be mixed with biofactories. After crosslinking, it supports bacterial viability and metabolic activity for at least three weeks while containing their proliferation to the volume of the ring. Our experiments showed 7 days HA release in a tunable and sustained manner. This approach represents a sustainable alternative for long-term lubrication and might allow extended wear and greater comfort of future CLs. However, systematic studies of HA release studies as function of bacteria density, hydrogel composition and nutrient concentration are required to fully understand and

control release profiles long term and their dependence on external conditions.

## 5. Experimental Section

**Materials:** PVA (Mowiol 18–88, 130 000 Da, 86.7–88.7% hydrolysis degree), NaOH, HCl, Lithium phenyl-2,4,6-trimethylbenzoylphosphinate (LAP) were purchased from Sigma Aldrich (USA). Divinyl sulfone (DVS) was purchased from Alfa Aesar (USA). STF was prepared in MilliQ water (pH 7.4) according to a protocol reported in a previous study.<sup>[52]</sup> The composition of the STF is described in Table S2 (Supporting Information). Nelfilcon A CLs were purchased from Alcon (Alcon Laboratories, USA).

**Methods:** <sup>1</sup>H-NMR spectra were recorded on a Bruker Avance 300 MHz. Gel permeation chromatography (GPC) was performed using a HPLC PSS GPC-MALLS System. Rheological and friction experiments were evaluated using a rotational rheometer DHR3 (TA Instruments) equipped with an OmniCure UV Source (Series 1500, 365–480 nm). An OmniCure UV light source with control unit (LX500) was used for crosslinking of hydrogels (420 nm, 6 mW cm<sup>-2</sup> for 2 min). An OCA 35 Optical Contact Angle Meter (Dataphysics) and an Abbebat multiwavelength refractometer (Anton-paar) were used for characterization of water contact angle and refractive index of the hydrogels. A Tecan Infinite M Plex multi-mode plate reader was used for transmittance, absorbance and bioluminescence measurements. Aqueous gel permeation chromatography/size exclusion chromatography (GPC-SEC) system (Agilent 1260 Infinity II Multi-Detector GPC/SEC equipped with ultraviolet, refractive index, light scattering, and viscosity detectors) was used to measure PVA and HA release from hydrogel supernatants. Microscope images were taken using Zeiss Cell Discoverer 7 microscope equipped with ZEISS LSM 900 and AiryScan 2 (Zeiss, Oberkochen, Germany) or Zeiss LSM-880 confocal laser scanning microscopy (Zeiss). Cell concentration in liquid cultures was quantified as optical density at 660 nm. High performance liquid chromatography (Agilent 1290 Infinity II, RI and UV detector) was used to quantify glucose and lactate from culture supernatant.

**Strain Engineering and Evaluation:** The wild type strain *C. glutamicum* DSM 20300 was obtained from the German Collection of Microorganisms and Cell Cultures (DSMZ, Braunschweig, Germany). HA-producing *C. glutamicum* derivatives were constructed through stepwise metabolic engineering. The *pClik int sacB* vector was used for genomic modification of *C. glutamicum*, and the *pClik 5a MCS* vector was used for episomal expression of genes of interest.<sup>[53]</sup> *Escherichia coli* strains DH5 $\alpha$  and NM522 were for vector amplification and methylation, prior to transformation of *C. glutamicum*. For the latter, the pTc plasmid was co-expressed in *E. coli* NM522. All strains and plasmids were stored in cryostocks at –80 °C. Cloning strategies were designed using SnapGene software (version 5.1.4.2, GSL Biotech LLC, Boston, MA, USA). Plasmid DNA was synthesized, purified, and analyzed as described previously.<sup>[54]</sup> In short, PCR was used to amplify desired DNA fragments from genomic DNA (Phusion High-Fidelity PCR Master Mix with HF Buffer, New England Biolabs, Frankfurt am Main, Germany) using specific primers. Vectors were linearized using Smal (FastDigest, Thermo Fisher Scientific, Waltham, MA, USA). The obtained fragments and the linearized vector backbone were assembled in vitro, and the obtained plasmids were transformed into *E. coli* by heat shock and into *C. glutamicum* by electroporation.<sup>[53]</sup> Correct clones were verified by PCR (Phire Green Hot Start II PCR Master Mix, Thermo Fisher Scientific) and Sanger sequencing (Azenta, Chelmsford, MA, USA).

To delete the *ldhA* gene (cg3219) encoding NAD-dependent L-lactate dehydrogenase (EC 1.1.1.27) from the genome, the upstream (570 bp) the downstream region (612 bp) of *ldhA* were amplified from genomic DNA. The fragments were then assembled in vitro with the linearized integrative vector. The vector was amplified and methylated in *E. coli*, isolated and then transformed into *C. glutamicum* DSM 20300. After two homologous recombination events, the desired deletion strain (*C. glutamicum*  $\Delta$ *ldhA*) was obtained. For episomal expression of the *hasA* and *hasB* genes from *Streptococcus equisimilis*,<sup>[55]</sup> encoding UDP-glucose dehydrogenase and HA synthase, respectively, a synthetic monocistronic operon based on digital sequence information (GenScript Biotech, Rijswijk, The

Netherlands) was synthesized. Genes were expressed under control of the two native promoter of the *P<sub>tuf</sub>* and *P<sub>sod</sub>* respectively, encoding elongation factor TU and previously shown to enable constitutive expression in *C. glutamicum*.<sup>[56]</sup> The two genes were separated by a 20 bp ribosomal binding site to enable efficient co-expression.<sup>[57]</sup> Insertion into the vector backbone yielded *pClik P<sub>tuf</sub> hasA P<sub>sod</sub> hasB*. To visualize the active expression of *hasAB* in suspended and encapsulated cells, the *mCherry* gene was used as a reporter.<sup>[58]</sup> For this purpose, the gene, together with a 20 bp ribosomal binding site, was cloned downstream of *hasAB* yielding the episomal vector *pClik P<sub>tuf</sub> hasA P<sub>sod</sub> HasB mCherry*. Further details on the cloning protocols can be taken from previous work.<sup>[59]</sup> Strains, plasmids, and primers, used in this study are summarized in Table S3 (Supporting Information).

The obtained strains were evaluated in liquid cultures for the desired phenotype. In the first step, *C. glutamicum* was precultured in BHI medium (37 g L<sup>-1</sup>, Brain heart Infusion, Becton Dickinson, Heidelberg, Germany). For subsequent precultures and main cultures, a minimal medium was used. Per liter, it contained 10 g of w, 15 g of (NH<sub>4</sub>)<sub>2</sub>SO<sub>4</sub>, 1 g of NaCl, 200 mg of MgSO<sub>4</sub>·7H<sub>2</sub>O, 55 mg of CaCl<sub>2</sub>, 20 mg of FeSO<sub>4</sub>·7H<sub>2</sub>O, 1 mg of thiamin HCl, 1 mg of calcium pantothenate, 0.5 mg of biotin, 100 mL of 2 M potassium phosphate buffer (pH 7.8), 10 mL of a trace element solution (200 mg L<sup>-1</sup> FeCl<sub>3</sub>·6H<sub>2</sub>O, 200 mg L<sup>-1</sup> MnSO<sub>4</sub>·H<sub>2</sub>O, 50 mg L<sup>-1</sup> ZnSO<sub>4</sub>·7H<sub>2</sub>O, 20 mg L<sup>-1</sup> CuCl<sub>2</sub>·2H<sub>2</sub>O, 20 mg L<sup>-1</sup> Na<sub>2</sub>B<sub>4</sub>O<sub>7</sub>·10H<sub>2</sub>O, 10 mg L<sup>-1</sup> (NH<sub>4</sub>)<sub>6</sub>Mo<sub>7</sub>O<sub>24</sub>·4H<sub>2</sub>O, adjusted to pH 1.0 with HCl), and 30  $\mu$ g L<sup>-1</sup> 3,4-dihydroxybenzoic acid. To maintain episomal plasmids, the medium was amended with 50  $\mu$ g mL<sup>-1</sup> kanamycin. For growth experiments, single colonies from BHI plates (20 g L<sup>-1</sup> Difco agar), preincubated at 30 °C for 48 h, were used to inoculate the first preculture (10 mL BHI medium in 100 mL baffled shake flasks), which was grown overnight on a rotary shaker (230 rpm, 85% humidity, Multitron, Infors AG, Bottmingen, Switzerland). Then, cells were harvested (3 min, 8800  $\times$  g, room temperature) and used to inoculate a second preculture in minimal medium (25 mL in a 250 mL baffled shake flask). Cells were harvested (3 min, 8800  $\times$  g, room temperature) during mid-exponential growth and used to inoculate the main cultures in minimal medium. These were inoculated in biological triplicate (50 mL medium in 500 mL baffled shake flasks) and incubated on an orbital shaker at 30 °C as given above. Growth, substrate consumption, and product formation were monitored over time. In addition, fluorescence microscopy was used to monitor the expression of mCherry.

**Bacterial Growth:** Cell growth was monitored as optical density at 660 nm using photometry.

**Glucose and Lactate Quantification:** Glucose and lactate were quantified by HPLC (1260 Infinity Series, Agilent Technologies) using an Aminex HPX-87H column (7.8 mm  $\times$  300 mm  $\times$  9  $\mu$ m, 55 °C, Bio-Rad Laboratories, Hercules, CA, USA) as the stationary phase and 3.5 mM H<sub>2</sub>SO<sub>4</sub> as the mobile phase (0.5 mL min<sup>-1</sup>). Glucose and lactate were measured using refractive index analysis (1260 RID, G1362A, Agilent Technologies), and their quantification was based on external standards.

**Chemical Functionalization of Poly(Vinyl Alcohol) (PVA) with Vinyl sulfone Groups (VS):** 4 g of PVA Mowiol 18–88 (130 kDa, 86.7–88.7% hydrolysis degree) were dissolved in water at 4% w/v by constant magnetic agitation at 90 °C for 4 h. NaOH was slowly added to get a final polymer concentration of 2% w/v in 0.1 M NaOH. A 1.5 molar excess of DVS with respect to the hydroxyl groups of PVA was added at room temperature under vigorous vortexing. The reaction was stopped after 1 min by adjusting the pH to 2 by dropping a 5 M HCl solution. The reaction mixture was purified by dialysis for 3 days against milli-Q water using a Spectra/Por Dialysis Membrane (MWCO: 3.5 kDa, Spectrum Laboratories, USA). After dialysis, the PVA-VS was freeze-dried and stored at rt. The degree of modification (DM) was quantified from the <sup>1</sup>H NMR spectrum in D<sub>2</sub>O (Figure S2b, Supporting Information) as the ratio between the integral of the signal corresponding to the vinyl protons from the VS groups ( $\delta$  = 6.9 ppm, 1H) and the signal corresponding to the methylene protons of the polymer backbone ( $\delta$  = 1.5 ppm, 2H) using MestReNova software (Mestrelab Research, Spain). The molecular weight of the purified PVA-VS was quantified by GPC (Figure S2c, Supporting Information) using 0.1 M NaCl and 30% MeOH as mobile phase at flow rate of 1 mL min<sup>-1</sup>.

Measurements were carried out at 35 °C and 51 bar. A column combination of PSS SUPREMA LUX precolumn (dimensions 8 × 50 mm<sup>2</sup>, particle size 10 μm) and a PSS SUPREMA Linear M (dimensions 8 × 300 mm<sup>2</sup>, particle size 10 μm) separation column was used. An RID Agilent detector with positive signal polarity was used at 35 °C. Pullulan–ReadyCal–Standards from PSS of molecular weights in the range of 180 Da to 1.39 MDa were used for the calibration. The sample injection volume was 100 μL.

**Preparation of Stock Solutions of PVA-VS and PVA:** Solutions of PVA-VS and PVA at 10% w/v concentration in water were prepared by heating at 90 °C for 4 h. Higher polymer concentrations did not render homogeneous solutions in water.

**Preparation of PVA-VS/PVA Hydrogels:** PVA-VS and PVA stock solutions were diluted to 5% w/v total polymer concentration. Variable PVA-VS/PVA ratio (95:5, 99:1, and 100:0) were prepared at room temperature by mixing the corresponding volumes of the stock solutions and diluting with a 1% w/v solution of LAP photoinitiator in BHI 2× medium. The concentration of LAP initiator in the final mixture was 0.5% w/v. For 10% w/v PVA-VS/PVA 100:0 hydrogels, LAP was directly added to the PVA-VS stock solution in a 0.5% w/v concentration. The precursor solutions were vortexed for 10 min, transferred to a mold (37 μL) of 12 mm diameter, and photocrosslinked with a UV light source (365–480 nm) at irradiance of 6 mW cm<sup>-2</sup> for 2 min. Flat hydrogel discs of 12 mm diameter and 300 μm thickness were obtained.

**Preparation of Bacterial-PVA-VS/PVA Hydrogels:** *C. glutamicum* was inoculated and cultured in BHI supplemented with 50 μg mL<sup>-1</sup> of kanamycin overnight at 30 °C. A subculture with OD600 0.01 was isolated for 4 h before encapsulation. The bacterial suspension in BHI 2× medium was mixed with 10% w/v aqueous stock solutions of PVA-VS and PVA with PVA-VS/PVA 95:5 ratio and a LAP photoinitiator solution to obtain a 5% w/v total polymer concentration, 0.5% w/v LAP initiator and an OD600 of 0.05 (≈4 × 10<sup>6</sup> cells mL<sup>-1</sup>). The polymer/bacteria suspension was vortexed for 1 min, transferred to a mold, and photocrosslinked as specified in the previous section.

**Rheological Properties:** The rheological properties of PVA/PVA-VS hydrogels were evaluated using a rotational rheometer equipped with UV Source (365–480 nm, 6 mW cm<sup>-2</sup>). A 20 mm Peltier UV transparent bottom plate and a smooth stainless steel 12 mm top plate geometry were used. Measurements were performed at room temperature using 37 μL of the hydrogel precursor solution and 300 μm gap between plates. Samples were sealed with silicon oil for the measurements and a solvent trap was used to avoid water evaporation. Strain sweep oscillatory experiments recorded from 0.001% to 1000% at a constant frequency of 1 Hz, and frequency sweep oscillatory experiments performed from 0.01 to 100 Hz at a constant strain of 0.1%, were tested to determine the linear viscoelastic region of PVA-VS/PVA hydrogels 15 min after preparation (Figure S3c,d, Supporting Information). Time sweep oscillatory experiments of PVA-VS/PVA solutions were performed to monitor mechanical properties. For that, samples were irradiated at 6 mW cm<sup>-2</sup> after 80 s of experiment for 120 s at 0.1% strain and 1 Hz frequency (found to be in the linear viscoelastic region), and the changes in the storage or elastic (*G'*) and the loss or viscous (*G''*) moduli were monitored for 3.5 min (Figure S3a, Supporting Information). *G'* and *G''* at 0.1% strain and 1 Hz frequency were also monitored for the commercial Focus Dailies CLs (Table 1). All the experiments were performed in triplicate.

**Equilibrium Water Content (EWC) and Oxygen Permeability:** The EWC and oxygen permeability of PVA-VS/PVA hydrogel discs and the commercial Focus Dailies CLs were evaluated. PVA-VS/PVA flat hydrogel discs of 12 mm diameter and 300 μm height (37 μL of polymer precursor solution) were prepared by molding as previously explained. Hydrogel samples were dried at 60 °C for 4 h and the weight of the dried hydrogels (*W<sub>d</sub>*) was recorded. Dried hydrogels were then submerged in 1.5 mL of STF for 24 h at 30 °C. After incubation, the hydrated samples were blotted using filter paper and weighted (*W<sub>t</sub>*) again. The percentage of EWC was calculated using Equation (1):

$$\text{EWC (\%)} = \frac{W_t - W_d}{W_t} \times 100 \quad (1)$$

Measurements were done in triplicate and average and standard deviation were given. The oxygen permeability, indicated as *D<sub>k</sub>*, where “*D*” is the diffusivity of the lens and “*k*” is the oxygen solubility in the material, were calculated according to Equations (1) and (2):<sup>[60,61]</sup>

$$D_k = 1.67e^{0.0397EWC} \quad (2)$$

**Water Contact Angle:** Water contact angle measurements of PVA/PVA-VS hydrogel discs and commercial Focus Dailies CLs were performed using an OCA 35 Optical Contact Angle Meter (Dataphysics) and the sessile drop method. PVA-VS/PVA flat hydrogel discs of 12 mm diameter and 300 μm height (37 μL of polymer precursor solution) were prepared by molding as previously explained. A 2 μL water droplet was deposited on the surface of the sample at room temperature and a side-view photo was taken to determine the contact angle. Measurements were performed at least in triplicate and average and standard deviation is given.

**Optical Transmittance:** PVA-VS/PVA hydrogels (40 μL of polymer precursor solution) were prepared from stock solutions by molding into a transparent, flat-bottom, 96-well plate by photocrosslinking with a UV light source (420 nm) at irradiance of 6 mW cm<sup>-2</sup> for 2 min. Optical transmittance of the hydrogels was measured with a plate reader. Measurements were performed after hydrogel preparation, and after incubation for 2 and 24 h of in STF at 30 °C (Figure S13, Supporting Information). Absorbance scans were taken at wavelengths from 400 to 800 nm at 5 nm increments and optical transmittance was calculated from the absorbance readings. Values at 600 nm (representative point of the visible spectrum range) are given in Table 1. Measurements were done in quadruplets and average and standard deviations were given.

**Refractive Index:** PVA-VS/PVA flat hydrogel discs of 12 mm diameter and 300 μm height (37 μL of polymer precursor solution) were prepared by molding as explained above. Hydrogel samples prepared and the commercial Focus Dailies CLs were incubated in STF for 24 h at 30 °C. The refractive index of the hydrated samples at 589.3 nm was measured and is presented in Table 1.

**Quantification of PVA Release:** PVA-VS/PVA flat hydrogel discs of 12 mm diameter and 300 μm height (37 μL of polymer precursor solution) were prepared by molding as previously explained and immersed in 1.5 mL of STF at 30 °C. After specific time points (3, 5, 7, 14, and 21 days) supernatants were collected and evaluated using GPC-SEC system. The injection volume was 100 μL. A mobile phase comprising HPLC grade water was used at a flow rate of 1 mL min<sup>-1</sup>. A PL aquagel-OH MIXED-H 8 μm, 7.5 × 300 mm SEC column (part number: PL2080-0700) was used with a particle size of 8 μm and a molecular weight range of 6–10 000 kDa. The InfinityLab EasiVial PEO/PEG standards with *M<sub>w</sub>* of 61–1608 kDa, 19.4–1046 kDa, 10.6–545 kDa, and 85.2 kDa were used for column calibration. A calibration curve of PVA was performed with PVA Mowiol 18–88 solutions at 1.0, 0.5, 0.2, 0.1, 0.05 mg mL<sup>-1</sup>. Measurements were done at least in triplicate and average and standard deviation were given. Analysis of variance (ANOVA) using Tukey grouping method of the results for PVA release from PVA-VS/PVA 99:1 and 95:5 hydrogels was performed at a significant level of \**p* < 0.05.

**Quantification of Diffusion Properties:** PVA-VS/PVA hydrogels in the ratios 95:5 and 100:0 at 5% w/v, and 100:0 ratio at 10% w/v, were prepared on the bottom of a transwell insert (Falcon Cell Culture Inserts, transparent PET membrane 8.0 μm pore size). For this, 45 μL of hydrogel precursor solutions (prepared as previously explained) were pipetted into the transwell insert and crosslinked (405 nm, 6 mW cm<sup>-2</sup>, 2 min), obtaining hydrogels with 6.3 mm diameter and ≈1 mm thickness. The transwell inserts containing the hydrogel were placed on a 24-well plate containing 700 μL of buffer (DPBS1x buffer without CaCl<sub>2</sub> or MgCl<sub>2</sub>). A solution containing the following proteins was prepared: Aldolase rabbit 160 kDa, Albumin bovine 67 kDa, Albumin egg 45 kDa, Chymotrypsinogen A 25 kDa, Myoglobin equine 17.8 kDa, Cytochrome C 12.3 kDa (SERVA, Germany). The protein solution was prepared in the same buffer at equimolar ratio of 5.5 μM for each protein, and with a total protein concentration of 1 mg mL<sup>-1</sup>. 200 μL of the protein solution were loaded on the top of the inserts. The hydrogel samples were incubated at 30 °C for 21 days. At defined incubation times (1, 2, 3, 7, 10, 14, 21 days), a 25 μL aliquot was collected from the bottom

of each well and 25  $\mu\text{L}$  of DPBS1x buffer was added to maintain the total volume unmodified. The set-up is illustrated in Figure S5a (Supporting Information). Protein quantification was calculated by using the Bicinchoninic acid (BCA) assay (Pierce BCA Protein Assay Kit, Thermo Scientific) with a plate reader (562 nm) and using a calibration curve. The calibration curve was obtained by measuring the absorbance of a set of bovine serum albumin (BSA) standard solutions (concentration range from 25 to 2000  $\mu\text{g mL}^{-1}$ , prepared in DPBS1x buffer) treated with the BCA assay kit protocol at 562 nm. Measurements were done at least in triplicate and average and standard deviation were given. The collected samples were analyzed by sodium dodecyl sulfate-polyacrylamide gel electrophoresis (SDS-PAGE) to evaluate the molecular weight of the diffused proteins (Figure S5b, Supporting Information). 15  $\mu\text{L}$  of each sample were firstly mixed with 5  $\mu\text{L}$  of 4 $\times$  Laemmli sample buffer, and incubated at 98  $^{\circ}\text{C}$  for 10 min, followed by cooling down to 4  $^{\circ}\text{C}$  in a thermocycler PCR instrument, to denature the proteins. Resulting denatured samples and a reference ladder of protein standards (Thermo Fisher, NEB P7718S9) were loaded into a 13% w/w polyacrylamide resolving gel. Electrophoresis was performed at 100 V, in 1 $\times$  running buffer (obtained by dilution in milli-Q water of 10 $\times$  running buffer: 1% w/w Tris-HCl, 1.92 M Glycine, 0.25 M SDS in milli-Q water) at room temperature, for  $\approx$ 90 min, until the dye front reached the bottom of the resolving gel. The resolved gels were rinsed thrice with milli-Q water and then stained by incubation in 50 mL of Coomassie Brilliant Blue Dye (Bio-Rad) for 1 h at room temperature, followed by destaining in milli-Q water overnight at room temperature. For image acquisition, the destained gels were analyzed in Gel-Doc (Cell Biosciences) with Flourescence Q software.

**Bacterial Viability:** Bacterial PVA-VS/PVA 95:5 hydrogels (10  $\mu\text{L}$ ) were prepared in  $\mu$ -Slide Angiogenesis well-plates (Ibidi, Munchen, Germany) and incubated with BHI medium at 30  $^{\circ}\text{C}$  for 21 days. The medium was changed every 7 days. The LIVE/DEAD BacLight Bacterial Viability assay (Thermo Fisher Scientific L7012) was used following manufacturer instructions to stain the encapsulated bacteria inside the hydrogels. At specific time points (0, 3, 7, 14, and 21 days), the supernatant was removed and replaced by DPBS1x containing the live/dead staining reagent. Samples were imaged in the following 2 h using a Zeiss Cell Discoverer 7 microscope equipped with ZEISS LSM 900 and AiryScan 2 (Zeiss, Oberkochen, Germany). Images were captured using AiryScan mode with Zeiss Plan-Apochromat 20 $\times$ /0.95 objective, optovar 1 $\times$  Tubelens lens. Excitation/Emission was set at 488 nm/450–555 nm and 561 nm/450–700 nm respectively for live and dead bacterial populations. Images of a size of ( $xy$ ) 132.12  $\times$  132.12  $\mu\text{m}$  (1328  $\times$  1328 pixels), and a Z-stack of 18  $\mu\text{m}$  were taken in the center of the hydrogels and 10–30  $\mu\text{m}$  above the plate surface for all the samples using ZEN 3.6 Blue software (Zeiss).  $N = 2$ , experiments were performed at least in triplicate, average and standard deviation were given, and at least 3 different images per sample were taken. The Imaris Surface module (Imaris v9.8, Bitplane, Zurich, Switzerland) was used to calculate the volume fraction of live and dead bacterial colonies. All images were pre-processed using background subtraction before an automatic threshold was applied to create surfaces for live and dead colonies (Imaris). The volume fraction of either live or dead bacteria using Imaris.

**ATP Quantification:** Bacterial PVA-VS/PVA 95:5 hydrogels (40  $\mu\text{L}$ ) were prepared in opaque all-white 96-well plates and 300  $\mu\text{L}$  of BHI medium were added on top of each hydrogel. Samples were incubated at 30  $^{\circ}\text{C}$  for different time points (from 3 h to 21 days) and medium was changed every 7 days. The CellTiter-Glo 3D Cell Viability Assay (Promega, USA) was used to determine the amount of ATP of the encapsulated bacteria inside the hydrogels. At each specific time point, medium was removed from the hydrogels and the CellTiter-Glo 3D reagent was added to the samples following manufacturer's protocol. After 30 min of incubation in the dark at room temperature while shaking, the luminescence of the sample was measured using a multi-mode plate reader. As a control, empty hydrogels and bacterial suspensions were cultured and analyzed under the same conditions.  $N = 2$ , experiments were performed at least in triplicate, and average and standard deviation were given. ATP quantification of bacteria encapsulated in PVA-VS/PVA 100:0 and 95:5 hydrogels during incubation for 7 days in BHI medium was also tested using the same methodology.  $N = 1$ , the ex-

periment was performed at least in triplicate, and average and standard deviation are given.

**Test for Bacteria Release from Living Hydrogels:** 2  $\mu\text{L}$  of the supernatant of bacterial hydrogels were streaked on agar plates prepared with BHI medium and 50  $\mu\text{g mL}^{-1}$  of Kanamycin and incubated at 30  $^{\circ}\text{C}$  for 48 h to check if they contained bacteria. Negative control corresponds to BHI medium, and positive control corresponds to a bacterial suspension (OD600 0.05) in BHI medium.

**Bacterial HA Production and Release:** GPC was used to measure cumulative HA concentration in supernatant samples from bacterial suspensions and from the growth activity experiment previously described; and supernatants of bacterial ring-CL prototype prepared and incubated as previously described. Extraction of HA from the supernatants was performed following a protocol adapted from previous works.<sup>[62,63]</sup> One volume of a 0.1% sodium dodecyl sulfate solution was added to the samples and incubated at 20  $^{\circ}\text{C}$  for 30 min to avoid polymer precipitation. Then, samples were centrifuged for 15 min at 15 000g, and the supernatant was mixed with two volumes of ice-cold ethanol (99%) for separation and precipitation of HA. Precipitation was carried out overnight at 4  $^{\circ}\text{C}$ . Samples were centrifuged a second time for 10 min at 10 000g to precipitate all the polymer, and the precipitated was redissolved in the same initial volume of HPLC grade ultrapure water. The final concentration and  $M_w$  range of HA in the samples was finally measured by GPC-SEC analysis with reflection index (RI), light scattering (LS), and viscometer (VS) detectors. The eluent used was HPLC grade ultrapure water. The system was operated at a temperature of 40  $^{\circ}\text{C}$ , with a flow rate of 1  $\text{mL min}^{-1}$  and an injection volume of 100  $\mu\text{L}$  was used. PL aquagel-OH MIXED-H 8  $\mu\text{m}$ , 7.5  $\times$  300 mm SEC column (part number: PL2080-0700) was used with a particle size of 8  $\mu\text{m}$  and a molecular weight range of 6–10 000 kDa. The InfinityLab EasiVial PEO/PEG with  $M_w$  of 61–1608 kDa, 19.4–1046 kDa, 10.6–545 kDa, and 85.2 kDa were used for column calibration. Calibration curves of HA and PVA were performed with HA standard solutions (Merck, Germany) with different molecular weights (10–30 kDa, 150–300 kDa, 500–750 kDa, 1500–1750 kDa, 1750–2000 kDa), and PVA Mowiol 18–88 solutions at 1.0, 0.5, 0.2, 0.1, 0.05  $\text{mg mL}^{-1}$ . To increase separation, the flow rate decreased to 0.8  $\text{mL min}^{-1}$  and the time was increased to 40 min in the method. Two peaks were observed in the chromatograms at different molecular weight ranges as observed in Figure S10 (Supporting Information), corresponding to the HA and PVA present in the supernatants. They were analyzed separately using the corresponding calibration curves for both polymers. Data for bacterial PVA-VS/PVA 95:5 hydrogels correspond to  $N = 1$  performed at least in triplicate, and average and standard deviation were given. Data for bacterial ring-CL prototypes correspond to  $N = 3$ , and average and standard deviation were given.

**Cell Culture:** Fibroblasts NIH-3T3 cells (from Swiss mouse embryonic fibroblasts in 1963) were purchased from DSMZ (Germany). The NIH-3T3 cells (passages between 6 and 13) were cultured in Dulbecco's Modified Eagle's Medium (DMEM) High Glucose (VWR, Germany) supplemented with 10% v/v fetal bovine serum (FBS) (PAN Biotech, Germany), 1.0% v/v GlutaMax (Gibco, Germany), and 1.0% v/v Penicillin/Streptomycin (Gibco, Germany). They were cultivated in T75 (75  $\text{cm}^2$ ) flasks and passaged below 70% cell confluency.

**Cytotoxicity of Bacterial Hydrogels:** NIH-3T3 cells were seeded in  $\mu$ -Plate Angiogenesis 96 well-plate (Ibidi, Germany) (16 000 cells  $\text{cm}^{-2}$ ) and grown for 24 h. Then, cell culture media was removed, cells were washed twice with DPBS, and they were fed with supernatants from the bacteria hydrogels diluted in supplemented DMEM (1:9 dilution). The analyzed samples correspond to supernatants from the ATP experiment and supernatants from bacteria ring-CL prepared and incubated as previously described.

After 24 h of incubation with the bacterial supernatant, the LDH assay was performed using the commercial kit CytoTox 96 Non-Radioactive (Promega) and following manufacturer's instructions. Briefly, equal volumes of the CytoTox 96 Reagent and supernatants (30  $\mu\text{L}$  each) were mixed and incubated at room temperature for 30 min on a shaker (300 rpm) in the dark. Then, 30  $\mu\text{L}$  of the stop solution from the assay kit was added and the absorbance at 490 nm ( $A_{490}$ ) was read using a plate reader (TECAN Spark). A negative control of cells cultured on normal growth medium,

and a positive control of cells treated with 2.5% Triton X-100 for lysing the cells (to induce 100% cell death) were also analyzed. The cell death percentage was obtained by taking the ratio of  $A_{490}$  of background-corrected samples and the average of  $A_{490}$  of background-corrected positive controls and multiplying them by 100. Data for bacterial PVA-VS/PVA 95:5 hydrogels correspond to  $N = 1$  performed at least in triplicate, and average and standard deviation were given. Data for bacterial ring-CL prototypes correspond to  $N = 3$ , and average and standard deviation were given.

Alamar Blue assay was also performed on the samples. Alamar Blue reagent (10% v/v, Invitrogen) was added to the cells following the manufacturer's protocol. After 2 h of incubation, fluorescence (Ex/Em 570/600 nm) of medium was analyzed using a plate reader (TECAN Spark). A control of cells cultured on normal growth medium was also analyzed. Fluorescence values were normalized with the values of the control. Data for bacterial PVA-VS/PVA 95:5 hydrogels correspond to  $N = 1$  performed at least in triplicate, and average and standard deviation were given. Data for bacterial ring-CL prototypes correspond to  $N = 3$ , and average and standard deviation were given.

**Lysozyme Test:** Bacterial PVA-VS/PVA 95:5 hydrogels (10  $\mu$ L) were prepared in  $\mu$ -Slide Angiogenesis well-plates (Ibidi, Munchen, Germany) and incubated with lysozyme (Carl Roth 8259.2, Lysozyme  $\approx 14\,000\text{ g mol}^{-1}$ , salt-free and albumin-free lyophilized powder) solutions at 0.65, 1.855, and 5.55 mg mL<sup>-1</sup> in BHI medium at 30 °C for 24 h. Samples incubated in BHI medium were taken as a control. The LIVE/DEAD BacLight Bacterial Viability assay (Thermo Fisher Scientific L7012) was then used to stain the encapsulated bacteria. Staining and imaging were carried out following the protocol previously described in bacterial viability section. The bacterial survival rate was calculated as the percentage of live bacteria considering the total number of bacteria observed in the fluorescence images using Imaris software.  $N = 2$ , represented data were performed at least in triplicate, and average and standard deviation are given.

**Quantification of the Friction Coefficient:** The friction force of PVA-VS/PVA hydrogel discs and commercial PVA-based CL (Focus Dailies, Alcon) was measured at 25 °C using a rotational rheometer with a Peltier plate following a reported methodology.<sup>[30,31]</sup> PVA-VS/PVA 95:5 hydrogel discs at 5% w/v concentration without bacteria and containing *C.*<sup>[31,32]</sup> PVA-VS/PVA 95:5 hydrogel discs at 5% w/v concentration without bacteria and containing *C. glutamicum* wild type or HA-producer *C. glutamicum*, were prepared as described in previous sections. Discs were then incubated in BHI medium at 30 °C and the friction force was measured after specific times of incubation (0, 1, and 7 days) in the presence of the supernatant. The friction force of the commercial CLs was measured in the presence of STF and supernatant of PVA-VS/PVA 95:5 hydrogel containing *Corynebacterium* producing HA after 7 days of incubation. The surface of the hydrogels (12 mm diameter) was blotted using filter paper and glued to a 40 mm steel plate geometry with Loctite Super Glue 406 (Spain). 500  $\mu$ L of the corresponding supernatant were added on the Peltier plate and the geometry was moved toward the plate until an initial gap of 300  $\mu$ m was reached. First, a 15 min conditioning step was carried out to avoid the influence of relaxation on the measurement. Then, a peak hold step with an angular velocity ( $\omega$ ) of 0.05 rad s<sup>-1</sup> was performed for 15 min at a strain-constant mode, and the torque ( $T$ ) and the normal force ( $W$ ) were detected. The obtained torque is a total value over the velocity range from 0 to  $\omega R$ , where  $R$  is the radius of the gel disc, as the velocity changes with the distance from the center of the axis. Therefore, the total frictional force ( $F$ ) and the coefficient of friction ( $\mu$ ) were determined as follows using Equations (3) and (4):<sup>[64]</sup>

$$F = \frac{4T}{3R} \quad (3)$$

$$\mu = \frac{F}{W} \quad (4)$$

Two independent experiments ( $N = 2$ ) were performed. Represented data were performed at least in duplicate, and average and standard deviation

are given. One sample per group was discarded because of handling problems.

**Fabrication of CL Prototype:** A two-step molding process was used, as illustrated in Figure 5a. 20  $\mu$ L of bacterial polymer precursor solution PVA-VS/PVA 95:5 at 5% w/v concentration were placed into a ring-shape silicon mold (outside diameter 10 mm) and photocrosslinked (420 nm, 6 mW cm<sup>-2</sup>) for 2 min. The obtained ring-shape bacteria hydrogel was placed into a convex silicon mold (Figure S14, Supporting Information). 50  $\mu$ L of polymer precursor solution PVA-VS/PVA 100:0 at 10% w/v with 0.5% w/v LAP were dropped on the top (after sonication for 10 min) covering the external and internal part of the bacterial-hydrogel ring. The sample was photocrosslinked (420 nm, 6 mW cm<sup>-2</sup>) for 2 min. A convex hydrogel sample with diameter 11 mm containing the implanted ring of 1.5 mm thickness was detached from the mold. For better visualization, a ring-CL containing silica gel in the ring (50% w/w) was also fabricated (Figure 5b).

**Incubation of CL Prototype in Different Culture Conditions for HA Release Experiments:** CL prototypes were incubated in BHI medium at 30 °C for 3 days. Afterward, samples were either i) incubated in STF for 7 days and the supernatants were collected and replaced by fresh one each day, or ii) subjected to incubation/release cycles of 16 h in BHI and 8 h in STF respectively during 7. The STF supernatants from both scenarios were collected and analyzed for HA release by GPC, and for cytotoxicity studies. Live/Dead staining was performed after 7 days of incubation/release BHI/STF cycles and imaged using Zeiss LSM-880 confocal laser scanning microscopy (Zeiss) and Zeiss EC Plan-Neofluar 10x/0.30 M27 objective.

**Statistical Analysis:** All statistical analyses were performed with Origin software and values were presented as mean  $\pm$  SD. One-way analysis of variance (ANOVA) using the Tukey grouping method was used to analyze statistical differences of multifactorial comparisons. A probability value of  $p < 0.05$  was taken as statistically significant.

## Supporting Information

Supporting Information is available from the Wiley Online Library or from the author.

## Acknowledgements

The authors acknowledge funding from the Leibniz Association through the Leibniz Science Campus Living Therapeutic Materials. L.T.E. and A.d.C. acknowledge support from the German Science Foundation, SFB1028. The authors also acknowledge Dr. Petra Herbeck-Engel for her assistance in photographing the lens prototypes, contributing significantly to the visual documentation for this article; and M.Sc. Varun Tadimarri for his assistance in the analysis by gel electrophoresis, contributing to the preparation and imaging of the resulting gels.

Open access funding enabled and organized by Projekt DEAL.

## Conflict of Interest

The authors declare no conflict of interest.

## Data Availability Statement

The data that support the findings of this study are available from the corresponding author upon reasonable request.

## Keywords

hyaluronic acid, hydrogel, lubrication, smart contact lenses

Received: December 18, 2023

Revised: March 4, 2024

Published online: April 21, 2024

- [1] Y. Zhu, S. Li, J. Li, N. Falcone, Q. Cui, S. Shah, M. C. Hartel, N. Yu, P. Young, N. R. de Barros, *Adv. Mater.* **2022**, *34*, 2108389.
- [2] A. D. Pucker, A. A. Tichenor, *Clin. Optim.* **2020**, *12*, 85.
- [3] H. Sahabudeen, R. Machatschek, A. Lendlein, *Multifunct. Mater.* **2021**, *4*, 042001.
- [4] R. Patel, A Guide to Contact Lens Technologies, <https://www.optometryweb.com/Featured-Articles/567203-A-Guide-To-Contact-Lens-Technologies>, **2020**.
- [5] S. Kusama, K. Sato, S. Yoshida, M. Nishizawa, *Adv. Mater. Technol.* **2020**, *5*, 1900889.
- [6] Y. Zhu, R. Nasiri, E. Davoodi, S. Zhang, S. Saha, M. Linn, L. Jiang, R. Haghniaz, M. C. Hartel, V. Jucaud, *Small* **2023**, *19*, 2207017.
- [7] J. Mun, J. won Mok, S. Jeong, S. Cho, C.-K. Joo, S. K. Hahn, *RSC Adv.* **2019**, *9*, 16578.
- [8] E. B. Papas, *Ophthalmic Physiol. Opt.* **2021**, *41*, 1254.
- [9] J. Cui, D. Daniel, A. Grinthal, K. Lin, J. Aizenberg, *Nat. Mater.* **2015**, *14*, 790.
- [10] W. Lin, M. Kluzek, N. Iuster, E. Shimoni, N. Kampf, R. Goldberg, J. Klein, *Science* **2020**, *370*, 335.
- [11] S. Wolf, J. Becker, Y. Tsuge, H. Kawaguchi, A. Kondo, J. Marienhagen, M. Bott, V. F. Wendisch, C. Wittmann, *Essays Biochem.* **2021**, *65*, 197.
- [12] J. Becker, C. M. Rohles, C. Wittmann, *Metab. Eng.* **2018**, *50*, 122.
- [13] J. J. Messelink, F. Meyer, M. Bramkamp, C. P. Broedersz, *eLife* **2021**, *10*, e70106.
- [14] A. J. S. Leger, J. V. Desai, R. A. Drummond, A. Kugadas, F. Almaghrabi, P. Silver, K. Raychaudhuri, M. Gadjeva, Y. Iwakura, M. S. Lionakis, *Immunity* **2017**, *47*, 148.
- [15] A. J. St Leger, R. R. Caspi, *BioEssays* **2018**, *40*, 1800046.
- [16] B. Raudszus, D. Mulac, K. Langer, *Int. J. Pharm.* **2018**, *536*, 211.
- [17] N. Bühler, H.-P. Haerri, M. Hofmann, C. Irrgang, A. Mühlebach, B. Müller, F. Stockinger, *Chimia* **1999**, *53*, 269.
- [18] L. Wei, D. Zhou, X. Kang, *Innovative Food Sci. Emerging Technol.* **2021**, *71*, 102726.
- [19] E. M. Çanga, F. C. Dudak, *Carbohydr. Polym.* **2021**, *264*, 117990.
- [20] Y. Zhu, Z. Wang, L. Bai, J. Deng, Q. Zhou, *Mater. Des.* **2021**, *210*, 110018.
- [21] S. Bhusari, S. Sankaran, A. Del Campo, *Adv. Sci.* **2022**, *9*, 2106026.
- [22] X. Liu, H. Yuk, S. Lin, G. A. Parada, T. C. Tang, E. Tham, C. de la Fuente-Nunez, T. K. Lu, X. Zhao, *Adv. Mater.* **2018**, *30*, 1704821.
- [23] Z. Ming, L. Han, M. Bao, H. Zhu, S. Qiang, S. Xue, W. Liu, *Adv. Sci.* **2021**, *8*, 2102545.
- [24] P. Lambert, *J. Appl. Microbiol.* **2002**, *92*, 465.
- [25] S. Crouch, R. Kozlowski, K. Slater, J. Fletcher, *J. Immunol. Methods* **1993**, *160*, 81.
- [26] L. Kangas, M. Grönroos, A. Nieminen, *Med. Biol.* **1984**, *62*, 338.
- [27] H. Priks, T. Butelmann, A. Illarionov, T. G. Johnston, C. Fellin, T. Tamm, A. Nelson, R. Kumar, P.-J. Lahtvee, *ACS Appl. Bio Mater.* **2020**, *3*, 4273.
- [28] S. Sankaran, J. Becker, C. Wittmann, A. Del Campo, *Small* **2019**, *15*, 1804717.
- [29] P. Ren, T. Chen, N. Liu, W. Sun, G. Hu, Y. Yu, B. Yu, P. Ouyang, D. Liu, Y. Chen, *ACS Omega* **2020**, *5*, 33314.
- [30] D. Zhang, J. Shen, X. Peng, S. Gao, Z. Wang, H. Zhang, W. Sun, H. Niu, H. Ying, C. Zhu, *Front. Microbiol.* **2022**, *13*, 983545.
- [31] F. Yanez, A. Concheiro, C. Alvarez-Lorenzo, *Eur. J. Pharm. Biopharm.* **2008**, *69*, 1094.
- [32] J.-F. R. dos Santos, C. Alvarez-Lorenzo, M. Silva, L. Balsa, J. Couceiro, J.-J. Torres-Labandeira, A. Concheiro, *Biomaterials* **2009**, *30*, 1348.
- [33] J. P. Gong, Y. Osada, *Prog. Polym. Sci.* **2002**, *27*, 3.
- [34] N. B. Omali, L. N. Subbaraman, C. Coles-Brennan, Z. Fadli, L. W. Jones, *Optom. Vis. Sci.* **2015**, *92*, 750.
- [35] A. M. Bright, B. J. Tighe, *J. Br. Contact Lens Assoc.* **1993**, *16*, 57.
- [36] C. J. White, C. R. Thomas, M. E. Byrne, *Cont. Lens Anterior Eye* **2014**, *37*, 81.
- [37] A. Singh, P. Li, V. Beachley, P. McDonnell, J. H. Elisseeff, *Cont. Lens Anterior Eye* **2015**, *38*, 79.
- [38] F. A. Maulvi, A. A. Shaikh, D. H. Lakdawala, A. R. Desai, M. M. Pandya, S. S. Singhania, R. J. Vaidya, K. M. Ranch, B. A. Vyas, D. O. Shah, *Acta Biomater.* **2017**, *53*, 211.
- [39] M. Ali, M. E. Byrne, *Pharm. Res.* **2009**, *26*, 714.
- [40] A. Weeks, L. N. Subbaraman, L. Jones, H. Sheardown, *CLAOJ.* **2013**, *39*, 179.
- [41] F. A. Maulvi, T. G. Soni, D. O. Shah, *J. Biomater.* **2015**, *26*, 1035.
- [42] X. Zhang, X. Cao, P. Qi, *J. Biomater.* **2020**, *31*, 549.
- [43] R. C. Cooper, H. Yang, *J. Controlled Release* **2019**, *306*, 29.
- [44] A. R. Desai, F. A. Maulvi, M. M. Pandya, K. M. Ranch, B. A. Vyas, S. A. Shah, D. O. Shah, *Biomater. Sci.* **2018**, *6*, 1580.
- [45] F. A. Maulvi, S. S. Singhania, A. R. Desai, M. R. Shukla, A. S. Tannk, K. M. Ranch, B. A. Vyas, D. O. Shah, *Int. J. Pharm.* **2018**, *548*, 139.
- [46] A. R. Desai, F. A. Maulvi, D. M. Desai, M. R. Shukla, K. M. Ranch, B. A. Vyas, S. A. Shah, S. Sandeman, D. O. Shah, *Mater. Sci. Eng., C* **2020**, *112*, 110885.
- [47] E. Akbari, R. Imani, P. Shokrollahi, S. H. Keshel, *Macromol. Biosci.* **2021**, *21*, 2100043.
- [48] P. Hu, Q. Xie, C. Ma, G. Zhang, *Langmuir* **2020**, *36*, 2170.
- [49] H. Qiu, K. Feng, A. Gapeeva, K. Meurisch, S. Kaps, X. Li, L. Yu, Y. K. Mishra, R. Adelung, M. Baum, *Prog. Polym. Sci.* **2022**, *127*, 101516.
- [50] X. Liu, J.-L. Yang, D. Rittschof, J. S. Maki, J.-D. Gu, *Trends Ecol. Evol.* **2022**, *37*, 469.
- [51] M. Lejars, A. Margailan, C. Bressy, *Chem. Rev.* **2012**, *112*, 4347.
- [52] M. R. Marques, R. Loebenberg, M. Almukainzi, *Dissolution Technol.* **2011**, *18*, 15.
- [53] J. Becker, O. Zelder, S. Häfner, H. Schröder, C. Wittmann, *Metab. Eng.* **2011**, *13*, 159.
- [54] C. M. Rohles, G. Gießelmann, M. Kohlstedt, C. Wittmann, J. Becker, *Microb. Cell Fact.* **2016**, *15*, 154.
- [55] J. H. Sze, J. C. Brownlie, C. A. Love, *3 Biotech* **2016**, *6*, 67.
- [56] J. Becker, C. Klopprogge, O. Zelder, E. Heinzle, C. Wittmann, *Appl. Environ. Microbiol.* **2005**, *71*, 8587.
- [57] C. M. Rohles, L. Gläser, M. Kohlstedt, G. Gießelmann, S. Pearson, A. del Campo, J. Becker, C. Wittmann, *Green Chem.* **2018**, *20*, 4662.
- [58] M. Kohlstedt, S. Starck, N. Barton, J. Stolzenberger, M. Selzer, K. Mehlmann, R. Schneider, D. Pleissner, J. Rinkel, J. S. Dickschat, *Metab. Eng.* **2018**, *47*, 279.
- [59] F. Weiland, N. Barton, M. Kohlstedt, J. Becker, C. Wittmann, *Metab. Eng.* **2023**, *75*, 153.
- [60] X.-J. Zha, S.-T. Zhang, J.-H. Pu, X. Zhao, K. Ke, R.-Y. Bao, L. Bai, Z.-Y. Liu, M.-B. Yang, W. Yang, *ACS Appl. Mater. Interfaces* **2020**, *12*, 23514.
- [61] R. Moreddu, D. Vigolo, A. K. Yetisen, *Adv. Healthcare Mater.* **2019**, *8*, 1900368.
- [62] F. Cheng, H. Yu, G. Stephanopoulos, *Metab. Eng.* **2019**, *55*, 276.
- [63] C. D. Rodriguez-Marquez, S. Arteaga-Marin, A. Rivas-Sánchez, R. Autrique-Hernández, R. Castro-Muñoz, *Int. J. Mol. Sci.* **2022**, *23*, 6038.
- [64] J. P. Gong, G. Kagata, Y. Osada, *J. Phys. Chem. B* **1999**, *103*, 6007.